J|A|C|S ARTICLES

Published on Web 08/17/2009

Molecular Dynamics at Constant pH and Reduction Potential: Application to Cytochrome c_3

Miguel Machuqueiro† and António M. Baptista*

Instituto de Tecnologia Química e Biológica, Universidade Nova de Lisboa, Av. da República, EAN, 2780-157 Oeiras, Portugal

Received October 28, 2008; E-mail: baptista@itqb.unl.pl

Abstract: Here we present a new implementation and extension of the stochastic titration method which makes it possible to perform MD simulations at constant pH and reduction potential. The method was applied to the redox titration of cytochrome c_3 from *Desulfovibrio vulgaris* Hildenborough, and a major finding of this study was that the method showed a better performance when the protein region is assigned a high dielectric constant. This dependence on the value of the protein dielectric constant was not found in previous constant-pH MD simulations and is attributed to excessively high heme−heme interactions at low dielectric constants. The simulations revealed strong coupling between hemes in close proximity, and we also showed how these couplings can be used to estimate the sensibility of the heme reductions to small pH changes.

Introduction

It is well-known that redox processes, often coupled with protonation events, are essential for living organisms, being particularly important in respiration, photosynthesis, and other energy transduction systems. In terms of computational studies, two different and largely complementary approaches can be used to study reduction and protonation processes in proteins: molecular mechanics/dynamics (MM/MD),[1−16] where protein conformation changes are explicitly treated for a fixed ionization (protonation or reduction) state, and more simplified electrostatics-oriented methods (Poisson−Boltzmann (PB), generalized Born (GB), protein dipoles Langevin dipoles (PDLD), etc.),[17−30] where ionization changes are explicitly treated for a fixed protein conformation. The inherent complementarity of these two classes of methods, and their consequent incompleteness when taken individually, prompted several attempts to devise methods explicitly treating both conformation and ionization changes (e.g., see ref 31 for a succinct overview), eventually leading to the development of constant-pH MD methods.[31−>48] The theoretical aspects behind most constant-pH MD methods can in principle be extended to address also redox processes, so

† Current address: Department of Chemistry and Biochemistry, Faculty of Sciences, University of Lisbon, Campo Grande, Building C8, 1149-016 Lisbon, Portugal.

(1) Soares, C. M.; Martel, P. J.; Mendes, J.; Carrondo, M. A. *Biophys. J.* **1998**, *74*, 1708.
(2) Karplus, M.; Petsko, G. A. *Nature* **1990**, *347*, 631.
(3) van Gunsteren, W. F.; Berendsen, H. J. C. *Angew. Chem., Int. Ed. Engl.* **1990**, *29*, 992.
(4) Churg, A. K.; Warshel, A. *Biochemistry* **1986**, *25*, 1675.
(5) Cutler, R. L.; Davies, A. M.; Creighton, S.; Warshel, A.; Moore, G. R.; Smith, M.; Mauk, A. G. *Biochemistry* **1989**, *28*, 3188.
(6) Langen, R.; Jensen, G. M.; Jacob, U.; Stephens, P. J.; Warshel, A. *J. Biol. Chem.* **1992**, *267*, 25625.
(7) Langen, R.; Brayer, G. D.; Berghuis, A. M.; Mclendon, G.; Sherman, F.; Warshel, A. *J. Mol. Biol.* **1992**, *224*, 589.
(8) Mark, A. E.; van Gunsteren, W. F. *J. Mol. Biol.* **1994**, *240*, 167.
(9) Alden, R. G.; Parson, W. W.; Chu, Z. T.; Warshel, A. *J. Am. Chem. Soc.* **1995**, *117*, 12284.
(10) Apostolakis, J.; Muegge, I.; Ermler, U.; Fritzsch, G.; Knapp, E. W. *J. Am. Chem. Soc.* **1996**, *118*, 3743.
(11) Muegge, I.; Qi, P. X.; Wand, A. J.; Chu, Z. T.; Warshel, A. *J. Phys. Chem. B* **1997**, *101*, 825.
(12) Warshel, A. *Biochemistry* **1981**, *20*, 3167.
(13) Russell, S. T.; Warshel, A. *J. Mol. Biol.* **1985**, *185*, 389.
(14) Warshel, A.; Sussman, F.; King, G. *Biochemistry* **1986**, *25*, 8368.
(15) Lee, F. S.; Chu, Z. T.; Warshel, A. *J. Comput. Chem.* **1993**, *14*, 161.
(16) Del Buono, G. S.; Figueirido, F. E.; Levy, R. M. *Proteins Struct. Funct. Genet.* **1994**, *20*, 85.
(17) Sharp, K. A.; Honig, B. *Annu. Rev. Biophys. Biophys. Chem.* **1990**, *19*, 301.
(18) Honig, B.; Nicholls, A. *Science* **1995**, *268*, 1144.
(19) Martel, P. J.; Baptista, A. M.; Petersen, S. B. *Biotechnol. Annu. Rev.* **1996**, *2*, 315.
(20) Soares, C. M.; Martel, P. J.; Carrondo, M. A. *J. Biol. Inorg. Chem.* **1997**, *2*, 714.
(21) Baptista, A. M.; Martel, P. J.; Soares, C. M. *Biophys. J.* **1999**, *76*, 2978.
(22) Bashford, D.; Karplus, M.; Canters, G. W. *J. Mol. Biol.* **1988**, *203*, 507.
(23) Gunner, M. R.; Honig, B. *Proc. Natl. Acad. Sci. U.S.A.* **1991**, *88*, 9151.
(24) Bashford, D.; Karplus, M. *Biochemistry* **1990**, *29*, 10219.
(25) Bashford, D.; Gerwert, K. *J. Mol. Biol.* **1992**, *224*, 473.
(26) Bashford, D.; Case, D. A.; Dalvit, C.; Tennant, L.; Wright, P. E. *Biochemistry* **1993**, *32*, 8045.
(27) Yang, A. S.; Gunner, M. R.; Sampogna, R.; Sharp, K.; Honig, B. *Proteins Struct. Funct. Genet.* **1993**, *15*, 252.
(28) Demchuk, E.; Wade, R. C. *J. Phys. Chem.* **1996**, *100*, 17373.
(29) Warshel, A. *Biochemistry* **1981**, *20*, 3167.
(30) Lee, F. S.; Chu, Z. T.; Warshel, A. *J. Comput. Chem.* **1993**, *14*, 161.
(31) Baptista, A. M.; Teixeira, V. H.; Soares, C. M. *J. Chem. Phys.* **2002**, *117*, 4184.
(32) Mertz, J. E.; Pettitt, B. M. *Int. J. Supercomp. Ap* **1994**, *8*, 47.
(33) Baptista, A. M.; Martel, P. J.; Petersen, S. B. *Proteins Struct. Funct. Genet.* **1997**, *27*, 523.
(34) Machuqueiro, M.; Baptista, A. M. *J. Phys. Chem. B* **2006**, *110*, 2927.
(35) Machuqueiro, M.; Baptista, A. M. *Biophys. J.* **2007**, *92*, 1836.
(36) Machuqueiro, M.; Baptista, A. M. *Proteins Struct. Funct. Bioinf.* **2008**, *72*, 289.
(37) Borjesson, U.; Hunenberger, P. H. *J. Chem. Phys.* **2001**, *114*, 9706.
(38) Baptista, A. M. *J. Chem. Phys.* **2002**, *116*, 7766.
(39) Borjesson, U.; Hunenberger, P. H. *J. Phys. Chem. B* **2004**, *108*, 13551.
(48) Stern, H. A. *J. Chem. Phys.* **2007**, *126*, 164112.

10.1021/ja808463e CCC: $40.75

that MD simulations could reflect both the pH and the reduction potential (E) of the solution. A constant-(pH,E) MD method of this type would allow for the joint sampling of protein conformation, protonation, and reduction states, in a way that is impossible to obtain with current methods. However, to our knowledge, no such method has yet been reported. The central purpose of this work is thus to present a constant-(pH,E) MD method, based on the stochastic titration approach,[31] and apply it to a redox protein.

Several constant-pH MD methods rely on simplified electrostatic models to the fast calculation of ionization free energies[31,33−36,40−42,44−47] and their subsequent use to sample ionization states. In particular, the stochastic titration method[31] relies on the use of a PB model that treats the protein environment using a dielectric constant (ε_p), which is in general an empirical parameter accounting for contributions not explicitly included in the model.[49] The stochastic titration method treats atomic motion in a fully explicit way (via MM/MD), interpreting each PB calculation as referring to a hypothetical rigid protein.[31] This implies that ε_p should in principle account only for electronic polarization, meaning that a value around 2 should be used.[50] In practice, it has been shown that a higher ε_p does not improve the ability of the stochastic constant-pH MD method to predict the acidic pK_a's of hen egg white lysozyme (increasing ε_p just leads to nonsystematic differences of 0.1 in the overall rmsd of the pK_a values).[36] However, the nature of the reorganization of protein protonable and redox groups upon titration is considerably different, because structural rearrangement is much easier in the former (via side-chain torsion) than in the latter (usually lacking torsional freedom); e.g., in the case examined here (see below) the heme groups are tightly bound to the protein and able to reorganize only by means of very small global displacements, planar tilting or charge redistribution. Therefore, we decided to examine in the present work the dependence of the constant-(pH,E) MD simulations on the value of ε_p.

Desulfovibrio vulgaris Hildenborough cytochrome c_3 (DvHc_3) is a small (∼14 kDa) globular and monomeric tetraheme protein (Figure 1). It is constituted by 107 residues plus four hemes covalently bound to cysteines in the polypeptide chain together with bis-histidinyl axial ligation. DvHc_3 plays an important role in the periplasmatic metabolism of molecular hydrogen in sulfate-reducing bacteria,[51−53] acting as a mediator between the periplasmatic hydrogenase (the electron donor) and the high molecular weight cytochrome (the electron acceptor).[53−55] The four hemes are covalently held together in close proximity,

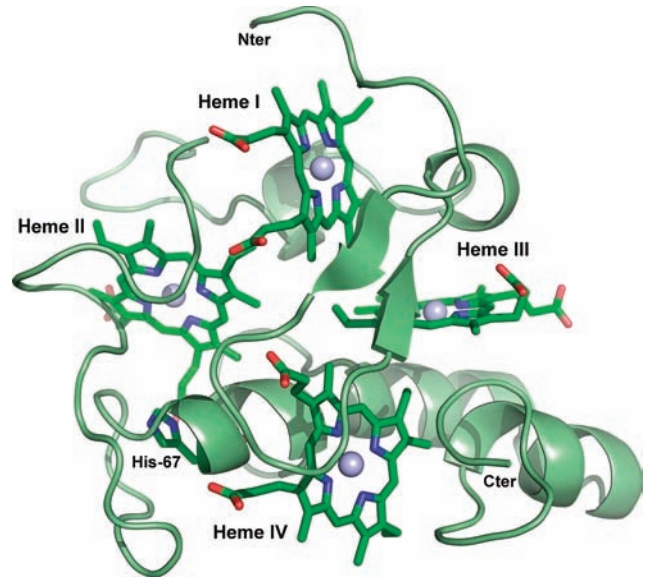

Figure 1. Structure of the DvHc_3 protein studied in this work. The main chain is shown as a cartoon and the heme groups as sticks. The figure was produced with PyMOL.[63]

exhibiting strong coupling between themselves and nearby acid/base groups, making heme reduction potential dependent on the oxidation state of the other three hemes (redox interaction potentials)[56−61] and on the pH (redox-Bohr effect).[62] If we also add up a very low residue to heme ratio, we obtain a tight densely packed structure where the heme reduction potentials are very close (within a range of 80 mV, or 1.3 pH units). This makes DvHc_3 an extremely demanding test case in terms of prediction, taking into consideration that 1.3 pH units is close to the constant-pH MD method pK_a prediction error previously reported.[36] Therefore, we decided to use this challenging system to test the performance of the constant-(pH,E) MD method presented here.

Computational Details and Methods

Constant-(pH,E) MD Method. The stochastic titration method originally developed to address protonation events[31] consists essentially of a piecewise MM/MD simulation in which the protonation states of the protein are periodically replaced with new states sampled by Monte Carlo using PB-derived free energy terms (see refs 31 and 34−36 for further details). The theoretical rationale of the method can be briefly stated as follows:[31] (a) MM/MD is assumed to correctly sample configurations for a fixed set of protonation states; (b) PB/MC is assumed to correctly sample

(40) Walczak, A. M.; Antosiewicz, J. M. *Phys. Rev. E* **2002**, 66.
(41) Dlugosz, M.; Antosiewicz, J. M.; Robertson, A. D. *Phys. Rev. E* **2004**, 69.
(42) Dlugosz, M.; Antosiewicz, J. M. *Chem. Phys.* **2004**, *302*, 161.
(43) Burgi, R.; Kollman, P. A.; van Gunsteren, W. F. *Proteins Struct. Funct. Genet.* **2002**, *47*, 469.
(44) Mongan, J.; Case, D. A.; McCammon, J. A. *J. Comput. Chem.* **2004**, *25*, 2038.
(45) Lee, M. S.; Salsbury, F. R.; Brooks, C. L. *Proteins Struct. Funct. Bioinf.* **2004**, *56*, 738.
(46) Khandogin, J.; Brooks, C. L. *Biophys. J.* **2005**, *89*, 141.
(47) Khandogin, J.; Brooks, C. L. *Biochemistry* **2006**, *45*, 9363.
(49) Schutz, C. N.; Warshel, A. *Proteins Struct. Funct. Genet.* **2001**, *44*, 400.
(50) Böttcher, C. J. F.; van Belle, O. C.; Bordewijk, P.; Rip, A. *Theory of electric polarization*; Elsevier: Amsterdam, 1973; Vol. I.
(51) Coutinho, I. B.; Xavier, A. V. *Methods Enzymol.* **1994**, *243*, 119.
(52) Pereira, I. A. C.; Teixeira, M.; Xavier, A. V. *Struct. Bonding (Berlin)* **1998**, *91*, 65.
(53) Pereira, I. A. C.; Romao, C. V.; Xavier, A. V.; LeGall, J.; Teixeira, M. *J. Biol. Inorg. Chem.* **1998**, *3*, 494.
(54) Yagi, T.; Honya, M.; Tamiya, N. *Biochim. Biophys. Acta* **1968**, *153*, 699.
(55) Aubert, C.; Brugna, M.; Dolla, A.; Bruschi, M.; Giudici-Orticoni, M. T. *Biochim. Biophys. Acta* **2000**, *1476*, 85.
(56) Santos, H.; Moura, J. J. G.; Moura, I.; Legall, J.; Xavier, A. V. *Eur. J. Biochem.* **1984**, *141*, 283.
(57) Coletta, M.; Catarino, T.; Legall, J.; Xavier, A. V. *Eur. J. Biochem.* **1991**, *202*, 1101.
(58) Turner, D. L.; Salgueiro, C. A.; Catarino, T.; Legall, J.; Xavier, A. V. *Biochim. Biophys. Acta* **1994**, *1187*, 232.
(59) Turner, D. L.; Salgueiro, C. A.; Catarino, T.; Legall, J.; Xavier, A. V. *Eur. J. Biochem.* **1996**, *241*, 723.
(60) Salgueiro, C. A.; Turner, D. L.; Xavier, A. V. *Eur. J. Biochem.* **1997**, *244*, 721.
(61) Louro, R. O.; Catarino, T.; Turner, D. L.; Picarra-Pereira, M. A.; Pacheco, I.; LeGall, J.; Xavier, A. V. *Biochemistry* **1998**, *37*, 15808.
(62) Papa, S.; Guerrieri, F.; Izzo, G. *Febs Lett.* **1979**, *105*, 213.
(63) DeLano, W. L. *The PyMOL Molecular graphics system*; DeLano Scientific: SanCarlos, CA, 2002;http://www.pymol.org.

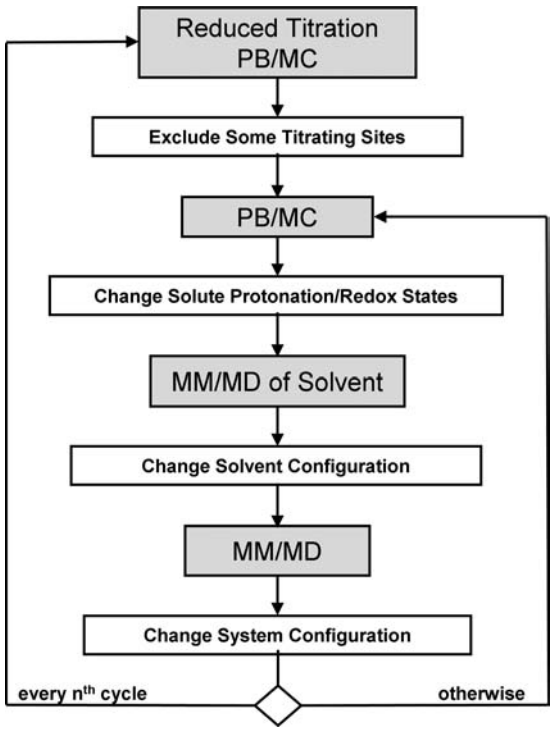

Figure 2. Schematic representation of the algorithm used.

protonation states for a fixed protein conformation; (c) using a standard theorem from the theory of Markov chains,[64] the succession of MM/MD and PB/MC simulations is then shown to produce a Markov chain which asymptotically samples from the proper semigrand canonical ensemble. Since the MM/MD simulations use explicit solvent while the PB/MC simulations use an automatically relaxed solvent (a dielectric continuum), a short MM/MD solvent relaxation is performed after selecting each new set of protonation states (see below), for consistency of the conditional distributions (this approximation is discussed in ref 31). The extension of the stochastic titration method to deal with reduction events is easily obtained by replacing the PB/MC sampling of protonation states in item (b) with the joint sampling of protonation *and* redox states.[21,65−69] Since this PB/MC joint sampling is in principle correct for a fixed protein conformation, the original proof in ref 31 necessarily holds if one replaces all occurrences of the protonation state with a general ionization (protonation + reduction) state; the inclusion of proton tautomerism is easily obtained in a similar way.[36] Therefore, the resulting stochastic titration procedure provides a sound method to perform MD simulations for given values of pH and reduction potential (E) of the solution.

The present implementation of the constant-(pH,E) MD method is a direct extension of our most recent implementation of the constant-pH MD method.[36] The method relies on different sequential blocks (Figure 2). The first block is a PB/MC calculation where the protonation/reduction states resulting from the last MC step are assigned to the protein. The second block is the solvent relaxation dynamics, a short MM/MD simulation of the system with frozen protein, which allows the solvent to adapt to the new protonation/reduction states (the duration of this block is hereafter designated as τ_{rlx}). The last block is a full MM/MD of the unconstrained system (the duration of this block is hereafter designated as τ_{prt}). A variant of the reduced titration method is used.[34−36,70] This reduced titration approach is particularly useful because it allows that sites fully (de)protonated at the simulated pH (or fully oxidized/reduced at the simulated reduction potential) are temporarily excluded from the calculations (the criteria is based on a cutoff value), hence strongly decreasing the computational cost. The inclusion of proton tautomerism on the protonable sites was done according to our previous work.[36] Thus, each titrable site can have each one of its proton locations empty/occupied, which results in two tautomers for His, three for the N-terminus, and four for the carboxylic acids of the propionates (each form, anti and syn, contributes with two tautomers). The treatment of heme groups is discussed below in the PB/MC and MM/MD subsections.

PB/MC Settings. The reduction potential of the heme model compound (E^{mod}) was initially taken as the value previously obtained in a rigid-structure PB/MC study (−249 mV)[66] but was subsequently adjusted to fit the experimental model (see the Results and Discussion). A value for E^{mod} cannot be easily inferred from the experimental model because the model compound does not correspond to a real molecule. Harbury et al. determined a reduction potential around −220 mV for an octapeptide bis-histidinyl derivative of the cytochrome c heme group,[71] but this value is affected by the particular environment (octapeptide and propionate groups) and can be regarded at best as an indicative value to our model compound. To avoid terminology misunderstandings, we stress that the E^{mod} value does *not* correspond to a heme group in the protein but to the hypothetical heme model compound in solution. The protein chemical environment around each heme group will in general be different and will lead to different values of the so-called intrinsic reduction potential, which refers to the titration of a single heme when all other sites are in some reference state (e.g., reduced and deprotonated) and is computed in the PB/MC method from the E^{mod} value and the electrostatic interactions with the protein environment. The terminology adopted here is the one of ref 21, which should be checked for further details.

PB calculations were performed with the program MEAD.[25] The atomic charges (excluding the heme group) and radii used in the PB calculations were derived from the GROMOS 43A1 force field[3,72] as previously described.[65] The heme group model compound and the partial charges used were the ones previously published;[73] in particular, the heme charges were calculated at the B3LYP level using the 6-31G(2df) basis set for the iron atom and 6-31G(d) for the remaining ones. All PB calculations consisted of finite-difference linear Poisson−Boltzmann calculations performed with the program MEAD (version 2.2.0)[25] using a temperature of 300 K, a molecular surface defined with a solvent probe radius of 1.4 Å, and a Stern (ion exclusion) layer of 2.0 Å. The dielectric constants were 80 for solvent and 2, 4, 8, and 15 for DvHc_3, depending on the system (see below), and the ionic strength was always 0.1 M. A two-step focusing procedure[74] was used, with consecutive grid spacing of 1.0 and 0.25 Å.

MC calculations were performed with the program PETIT.[21,67] The runs were performed using 10^5 MC cycles, one cycle consisting of sequential state changes over all individual sites and also all pairs of sites with at least one interaction term above 2.0 pK_a units (or 119 mV).[21]

(64) Feller, W. *An Introduction to Probability Theory and Its Applications*, 3rd ed.; Wiley: New York, 1968; Vol. I.
(65) Teixeira, V. H.; Cunha, C. A.; Machuqueiro, M.; Oliveira, A. S. F.; Victor, B. L.; Soares, C. M.; Baptista, A. A. *J. Phys. Chem. B* **2005**, *109*, 14691.
(66) Teixeira, V. H.; Soares, C. M.; Baptista, A. M. *J. Biol. Inorg. Chem.* **2002**, *7*, 200.
(67) Baptista, A. M.; Soares, C. M. *J. Phys. Chem. B* **2001**, *105*, 293.
(68) Mao, J. J.; Hauser, K.; Gunner, M. R. *Biochemistry* **2003**, *42*, 9829.
(69) Zhu, Z. Y.; Gunner, M. R. *Biochemistry* **2005**, *44*, 82.
(70) Bashford, D.; Karplus, M. *J. Phys. Chem.* **1991**, *95*, 9556.
(71) Harbury, H. A.; Cronin, J. R.; Fanger, M. W.; Hettinge, T. P.; Murphy, A. J.; Myer, Y. P.; Vinogradov, S. N. *Proc. Natl. Acad. Sci. U.S.A.* **1965**, *54*, 1658.
(72) Scott, W. R. P.; Hünenberger, P. H.; Tironi, I. G.; Mark, A. E.; Billeter, S. R.; Fennen, J.; Torda, A. E.; Huber, T.; Kruger, P.; van Gunsteren, W. F. *J. Phys. Chem. A* **1999**, *103*, 3596.
(73) Oliveira, A. S. F.; Teixeira, V. H.; Baptista, A. M.; Soares, C. M. *Biophys. J.* **2005**, *89*, 3919.
(74) Gilson, M. K.; Sharp, K. A.; Honig, B. H. *J. Comput. Chem.* **1988**, *9*, 327.

MM/MD Settings. All simulations were performed with the GROMOS 43A1 force field[3,72] for the GROMACS distribution[75,76] and with the SPC water model.[77] The heme parameters used were the ones previously published[73] (the same used in the present PB/MC calculations). Periodic boundary conditions were used, with a rhombic dodecahedral unit cell. Nonbonded interactions were calculated using a twin-range cutoff, with short- and long-range cutoffs of 8 and 14 Å, respectively, updated every five steps. Long-range electrostatics interactions were treated using the generalized-reaction-field method,[78] with an ionic strength value of 0.1 M[34] and an external dielectric constant of 54. Following our previous study comparing the performance of the generalized reaction field with and without ions,[34] no explicit ions were included in the simulations. All bond lengths were constrained using the LINCS algorithm,[79] and a time step of 2 fs was used. Two Berendsen's temperature couplings to baths at 300 K and relaxation times of 0.1 ps were used for both the solute and solvent.[80] A Berendsen's pressure coupling was used to scale the box, using a relaxation time of 2.0 ps and a compressibility of 4.5×10^{-5} bar^{-1}.[80]

The DvHc3 initial structure was the molecule labeled as "A" in the dimeric 2CTH entry[81] at the Brookhaven Protein Data Bank (PDB), corresponding to the fully oxidized form. The protein was placed at the center of a rhombic dodecahedral box, which was filled with 5899 water molecules. The minimum distance between images of DvHc3 was always higher than 20 Å. Two different setups were prepared where the heme groups were either fully oxidized or fully reduced. These two systems were minimized first with ~50 steps of steepest descent[82] followed by ~10000 steps using the l-bfgs (low-memory Broyden−Fletcher−Goldfarb−Shanno)[82] algorithm. The initializations were achieved by harmonically restraining all protein atoms in a 50 ps MD simulation, followed by another 50 ps simulation with only the CA atoms restrained. The resulting fully oxidized/reduced systems were used as the starting configuration for the simulations at potential values higher/lower than −300 mV.

Redox Titrations. The redox potential range studied was dependent on the ε_p value. The E values were as follows: −500, −450, −400, −350, and −300 mV for $\varepsilon_p = 2$; −420, −380, −350, −330, −310, −290, and −270 mV for ε_p 4; −380, −350, −330, −320, −310, −300, −290, −280, and −260 mV for $\varepsilon_p = 8$; and −350, −330, −310, −290, −270, −250, and −230 mV for $\varepsilon_p = 15$.

Runs of 10 ns (15 in case of $\varepsilon_p = 2$) were performed. Equilibrium is achieved within the first 5 (8 for $\varepsilon_p = 2$) ns, which were discarded in data analysis. Each redox potential setup was simulated with five different replicates, using different initial velocities. The relaxation of the solvent (τ_{rlx}) was done for 0.2 ps, while each full system dynamics segment (τ_{prt}) was 2.0 ps long.[34] All simulations were performed at pH 6.6, where all propionates, the N-terminus, and His67 were allowed to titrate. In agreement with previous rigid-structure PB/MC studies of DvHc3,[21,66] preliminary calculations showed that other potentially protonatable sites are not titrating at this pH value and were thus kept in their "standard" forms (charged Asp, Glu, Lys, Arg, and neutral Tyr). The titrating sites were treated in the current methodology taking into consideration their tautomeric forms.[26,36,46,47,67,83] A reduced titration method[34,70] was applied to the simulation every 100 ps using a cutoff of 0.001 (this means that titrations over 0.999 are set to 1 and titrations below 0.001 are set to 0 over the next 100 ps).

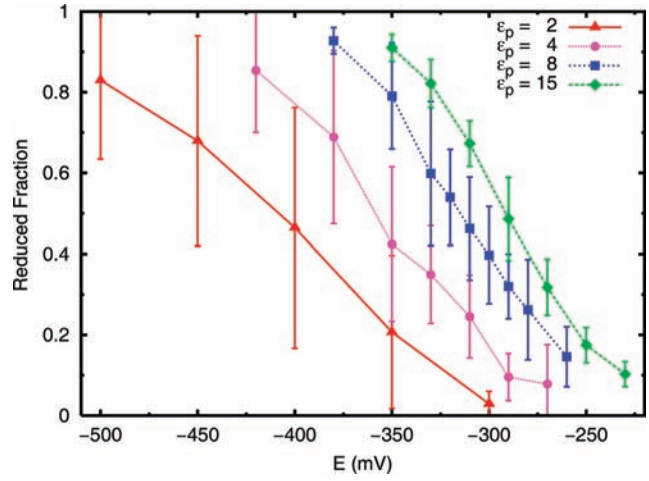

Figure 3. Redox titration curves at different ε_p values, using $E^{mod} = -249$ mV.

The heme redox titrations were computed by averaging at each redox potential value the occupancy states of all four sites over the final equilibrated segment. The data for each heme was fit to a Hill equation

$$f(E) = \{1 + \exp[n(E - E^{half})F/RT]\}^{-1}$$

where f is the reduction fraction, n is the Hill coefficient, F is the Faraday constant, and E^{half} is the midpoint reduction potential (i.e., the solution reduction potential for which the heme is half-reduced). This fit should be regarded as just a simple interpolation procedure to get the E value for which $f = 1/2$.

Analysis. The analysis of the simulations was done using GROMACS[75,76] or in-house tools. The calculations of correlation-corrected errors for averages over a single simulation replicate were computed using standard methods.[84] The final errors of the averages over replicates were computed using the law of total variance.

Results and Discussion

Redox Titration. The individual titration of each heme group could not be directly followed experimentally, but a simple model of five pairwise interacting sites (4 redox + 1 protonable) could be successfully fitted to the actual data.[59] Therefore, the results obtained with that experimental model will be used here to make all comparisons with our simulation results.

Since the heme groups in DvHc3 are all of the same type, our simulation results can be interpreted in terms of *relative* redox titrations. Thus, we could simply focus our attention on the differences between the reduction potentials of the four heme groups. Alternatively, the titrations derived from the experimental model can be easily fit by a shift of the reduction potential values, which corresponds to determining an "optimal" E^{mod} value. We decided to follow the latter route, which allows for an easier comparison with the experimental model.[59]

Figure 3 shows the total redox titration curves obtained for different ε_p values, using a previously determined E^{mod} value (see the Computational Details and Methods). In addition to

(75) Berendsen, H. J. C.; van der Spöel, D.; van Drunen, R. *Comput. Phys. Commun.* **1995**, *91*, 43.
(76) Lindahl, E.; Hess, B.; van der Spöel, D. *J. Mol. Model.* **2001**, *7*, 306.
(77) Hermans, J.; Berendsen, H. J. C.; van Gunsteren, W. F.; Postma, J. P. M. *Biopolymers* **1984**, *23*, 1513.
(78) Tironi, I. G.; Sperb, R.; Smith, P. E.; van Gunsteren, W. F. *J. Chem. Phys.* **1995**, *102*, 5451.
(79) Hess, B.; Bekker, H.; Berendsen, H. J. C.; Fraaije, J. G. E. M. *J. Comput. Chem.* **1997**, *18*, 1463.
(80) Berendsen, H. J. C.; Postma, J. P. M.; van Gunsteren, W. F.; Dinola, A.; Haak, J. R. *J. Chem. Phys.* **1984**, *81*, 3684.
(81) Simoes, P.; Matias, P. M.; Morais, J.; Wilson, K.; Dauter, Z.; Carrondo, M. A. *Inorg. Chim. Acta* **1998**, *273*, 213.
(82) Press, W. H.; Teukolsky, S. A.; Vetterling, W. T.; Flannery, B. P. *Numerical recipes in C, the art of scientific computing*, 2nd ed.; Cambridge University Press: New York, 1992.
(83) Alexov, E. G.; Gunner, M. R. *Biophys. J.* **1997**, *72*, 2075.
(84) Allen, M. P.; Tildesley, D. J. *Computer Simulations of Liquids*; Oxford University Press: New York, 1987.

the horizontal displacement of the curves, different ε_p values lead to considerably different slopes. This becomes clearer when the total titration curves are fit to those derived from the experimental model, as shown in Figure 4. The slope of the curves is obviously too small for $\varepsilon_p = 2$ and gradually increases with ε_p, ending up a bit too high at $\varepsilon_p = 15$. The too elongated titration curves at low ε_p reflect excessive interactions between the hemes, which are gradually attenuated by increasing ε_p. This is also evident from the individual heme midpoint reduction potentials (Table 1), with hemes I and III showing a large increase and decrease with ε_p, respectively. As a consequence, the total range of the E^{half} values decreases with ε_p, being closest to the value of the experimental model (80 mV) for $\varepsilon_p = 4$. The large interaction of the heme groups at low ε_p tends to shift their reductions to rather negative E values, making the best-fit E^{mod} values to vary considerably (from −259 to −126 mV) with ε_p. Furthermore, these results show that a good fit of the total titration curve does not necessarily correspond to a good prediction of the individual titrations, as already observed for the protonation case.[36]

As noted in the Introduction, DvHc3 is a very challenging test system because the range of the heme reduction potentials (~80 mV) is close to the error previously observed for pK_a values using the present stochastic titration methodology (~0.8 pH units).[36] As seen in Table 1, the root-mean-square deviation (rmsd) of the computed midpoint reduction potentials from the experimental model values is always similar to or lower than the ~0.8 pH units obtained for pK_a values. Nevertheless, given the close proximity of the experimentally derived reduction potentials, the rmsd values by themselves can be somewhat misleading in this case. An alternative or complementary approach is to look at the order of reduction of the hemes, shown in Table 2. At the higher ε_p values the reduction order is well reproduced except for heme III, which is always out of order. This need for higher ε_p values seems to indicate again a lack of reorganization effects in the simulations.

Overall, the above results seem to indicate that the system is exhibiting an incomplete reorganization upon heme reduction/oxidation during the simulations. The observed increase of heme interactions with the decrease of ε_p is what one would expect in a rigid-structure PB/MC study, where reorganization must be entirely captured by ε_p. Since structural reorganization does in principle occur explicitly (via MM/MD) in the present constant-(pH,E) MD method, it should not need to be accounted for by using a high ε_p. Indeed, the corresponding constant-pH MD method is not much affected by the ε_p value.[36] This discrepancy between protonable and redox groups may result from their different reorganization mechanisms, already noted in the Introduction. While protonable groups can achieve significant structural reorganization through side-chain torsion, the heme groups are structurally limited to planar tilting and to the small fluctuations allowed by the anchoring cysteines. On the other hand, the charge modifications associated with heme titration are much more spread than in typical protonatable groups, affecting the inner region of the porphyrin ring and the side chains of the coordinating histidines.[71] This can eventually result in a more extensive conformation−reduction coupling than would be anticipated from the heme structural hindrance and might end up affecting structural reorganization because of trapping or hysteresis effects.

However, the analysis of the simulations does not reveal any features suggesting insufficient structural reorganization. Figure 5 shows the temporal evolution of rmsd values near the half-

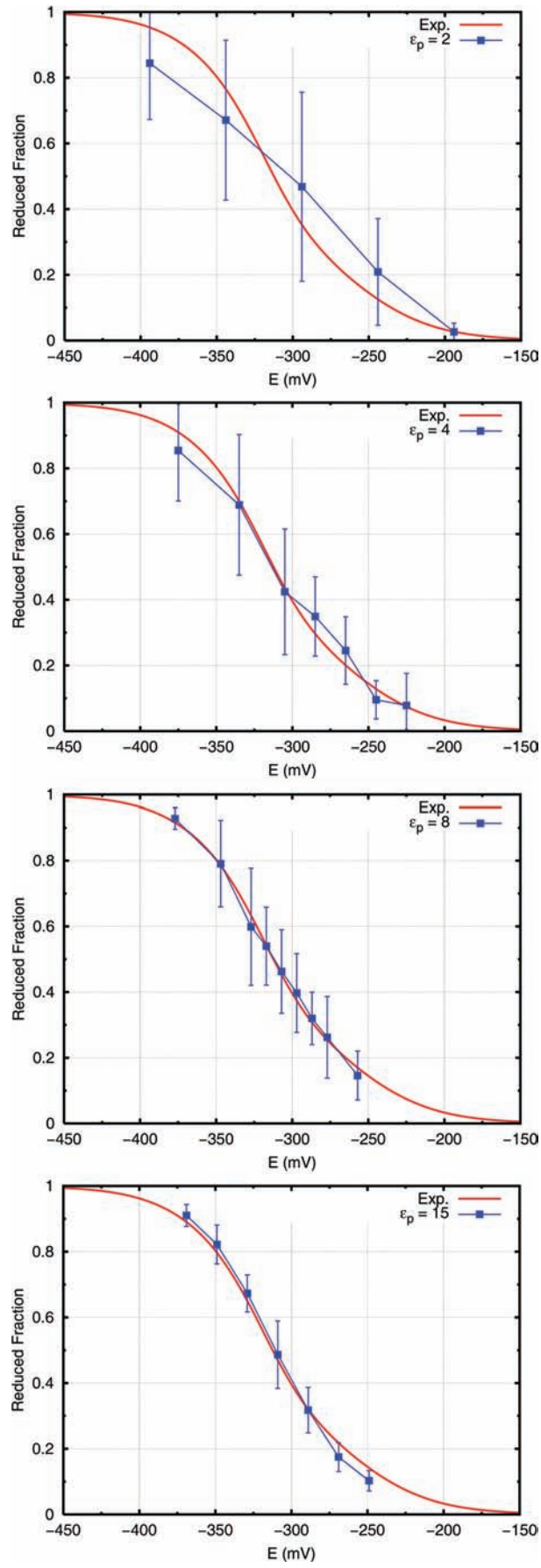

Figure 4. Total redox titration curves fitted to the experimental model.[59] The best E^{mod} values obtained from these fits are shown in Table 1.

Table 1. RMSD Values and Corresponding E^{mod} and E^{half} Obtained for Each ε_p

		E^{half} (mV)					rmsd	
ε_p	E^{mod} (mV)	heme I	heme II	heme III	heme IV	range	mV	pH units
2	−126	−360	−316	−243	−283	117	57	0.96
4	−193	−337	−321	−262	−280	75	43	0.73
8	−237	−312	−314	−286	−289	28	31	0.52
15	−259	−303	−312	−296	−291	21	27	0.45
expt[59]	−220[a]	−302	−307	−336	−256	80		

[a] Value corresponding to the reduction potential for an octapeptide bis-histidinyl derivative of the cytochrome c heme group.[71]

Table 2. Order of Reduction of the Heme Groups at Different ε_p Values

ε_p	low E ←					→ high E	
2	I	<	II	<	IV	<	III
4	I	<	II	<	IV	<	III
8	II	≤	I	<	IV	≤	III
15	II	<	I	<	III	≤	IV
exptl model	III	<	II	≤	I	<	IV

reduction of the cytochrome, showing that in all cases the protein remains stable and seems generally equilibrated after some nanoseconds. As intended, the different replicates are sampling somewhat different conformational regions. As shown in the Supporting Information, the protein secondary structure remains very stable during the simulations and the major differences to the X-ray structure are localized at a few regions. It is also important to note that the rmsd's obtained here must be higher than in a typical MD study; the X-ray structure refers to the fully oxidized state, while the constant-(pH,E) MD simulations are simultaneously sampling the conformation spaces corresponding to multiple combinations of redox and protonation states. Figure 6 shows the temporal evolution of the reduction fractions of the heme groups for one of the replicates shown in each plot of Figure 5. All hemes are effectively titrating at these E values, and none of them gets trapped at either the reduced or oxidized states. Figure 6 shows that the reduced/oxidized flips become more frequent as ε_p is increased, as expected, because increasing ε_p yields lower PB free energy differences and thus an easier switch between different oxidation states; the autocorrelation functions of the redox state (not shown) indicate correlation times around 0.5−1.0 ns for $\varepsilon_p = 2$, 0.2−0.5 for $\varepsilon_p = 4$, and below 0.1 ns for $\varepsilon_p = 8$ and 15. Overall, these results show that the coupling between conformation and reduction does not lead to trapping or hysteresis effects that could prevent a proper structural reorganization.

The above results suggest that the reorganization that seems to lack in the low-ε_p simulations is not of a structural nature. For example, the cumulative reduction of the closely packed hemes may involve some charge reorganization, which cannot be modeled using the present methodology. It is also interesting to note that the hemes whose behavior depends on ε_p (I and III) are the ones in close proximity to two other hemes (see Figure 1); hemes II and IV, which are in close proximity to only one other heme (and separated from each other by a helix), are essentially unaffected by the ε_p value. Furthermore, the behavior of the ε_p-dependent hemes is opposite: heme I is too difficult to reduce at low ε_p, where heme III is too easily reduced.

Since the data obtained using $\varepsilon_p = 8$ and 15 correctly predict the order of reduction of hemes I, II, and IV, they will be used in the remaining analysis.

Coupling between Sites. The analysis of the coupling between pairs of sites was done by computing the statistic correlations

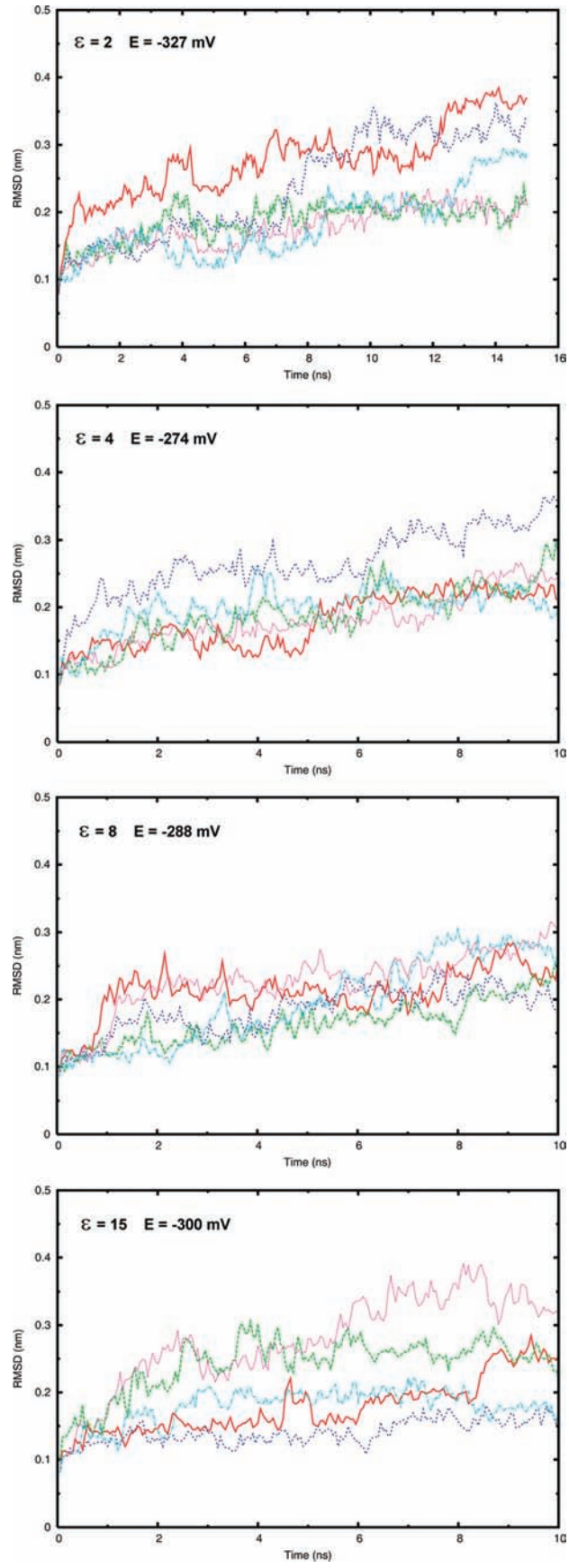

Figure 5. Temporal evolution of the root-mean-square deviation (rmsd) of the simulations near the half-reduction of cytochrome c_3, showing the five replicates at each ε_p value. The fit and rmsd values are computed using the C_α atoms and taken relative to the X-ray structure.

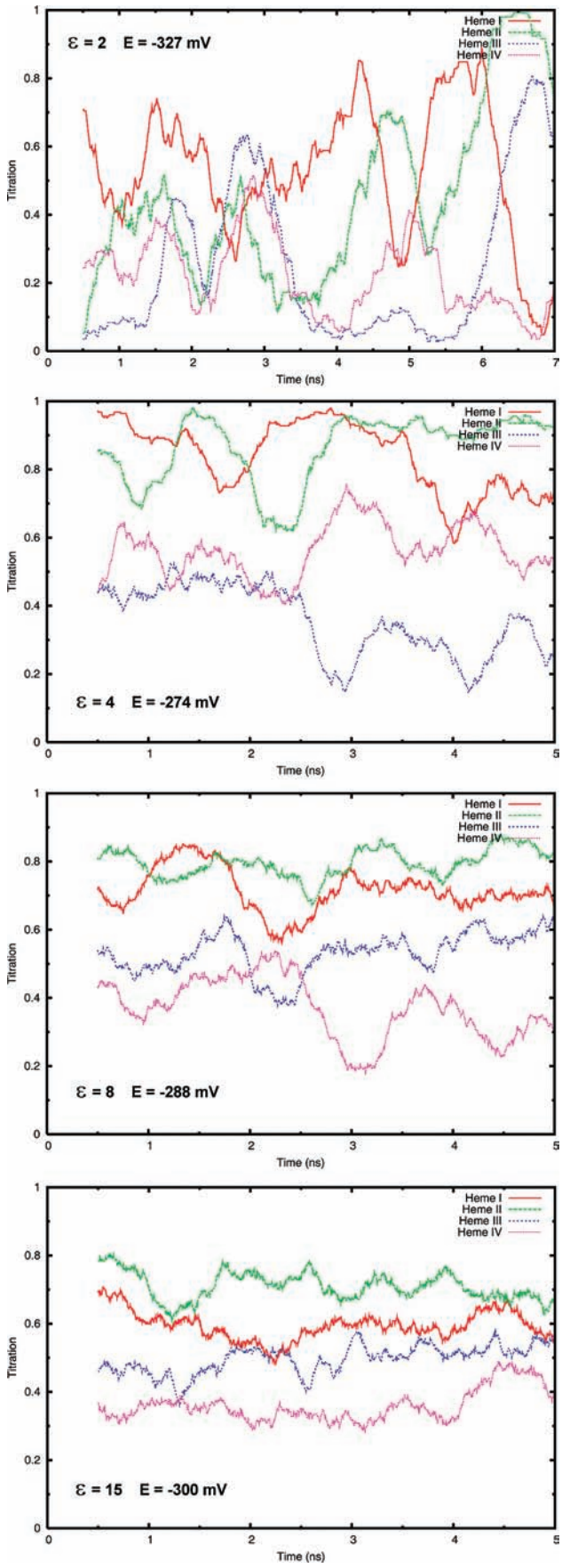

Figure 6. Temporal evolution of the shifting average (window size of 500 ps) of the reduction fraction of the hemes for different ε_p values. Each plot refers to one of the replicates shown in the corresponding plot of Figure 5.

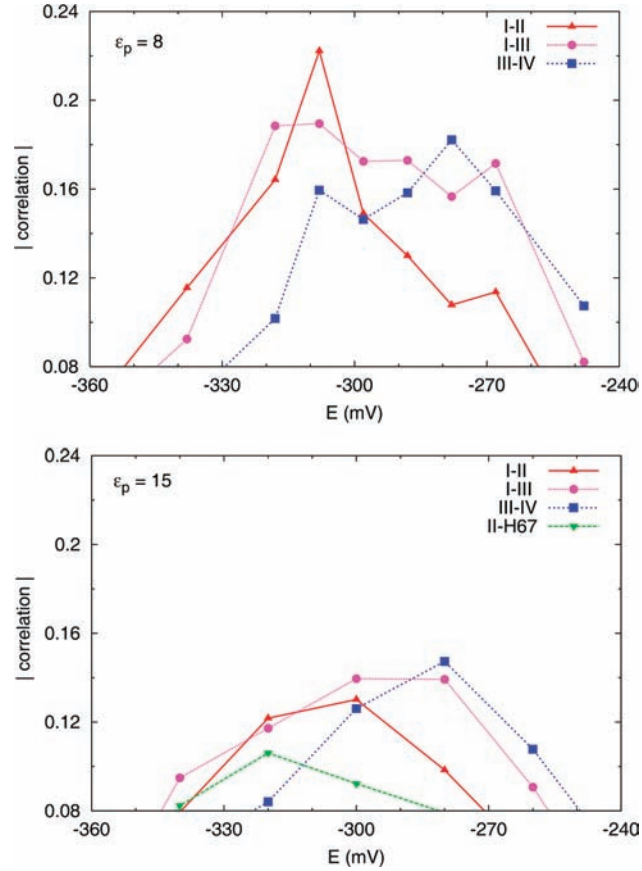

Figure 7. The absolute correlations between pairs of sites at $\varepsilon_p = 8$ and 15. All significant correlations have the sign expected from the direct interaction of the corresponding pair of sites (negative for heme−heme correlations and positive for heme−protonatable correlations).

of their occupancies,[21] given by

$$\mathrm{corr}(n_i,n_j) = (\langle n_i n_j\rangle - \langle n_i\rangle\langle n_j\rangle)/(\sigma(n_i)\sigma(n_j))$$

where n_i is the occupancy (0 or 1) of site i and the angle brackets and σ denote the ensemble averages and standard deviations, respectively. Two coupled sites with perfectly correlated occupancies should give a correlation of 1 (always occupied/occupied or empty/empty) or −1 (always occupied/empty or empty/occupied), while totally uncoupled/uncorrelated sites should give a correlation of zero.

Figure 7 shows all absolute correlations greater than 0.08, for $\varepsilon_p = 8$ and 15; lower ε_p values give similar profiles but with higher correlations (data not shown). Figure 7 shows that the stronger couplings are between the heme groups, in particular the pairs I−II, I−III, and III−IV. These pairs correspond to hemes in close proximity, while the absent pair corresponds to the more spaced-apart hemes II and IV (Figure 1). The correlations between these heme pairs are always negative, supporting the idea that they originate from direct interactions. Heme II also shows evidence of a relevant coupling with His67 which can be explained by their close proximity. When comparing these results with previous ones using rigid-structure PB/MC methodologies,[21,66] we see an excellent agreement between them. In the present simulations there are no significant correlations between the heme groups and their propionates (A and D) due to the fact that at pH 6.6 the propionates are hardly titrating. In general, the smoothness of the correlation curves (whose error is always higher than those of the averages) is a

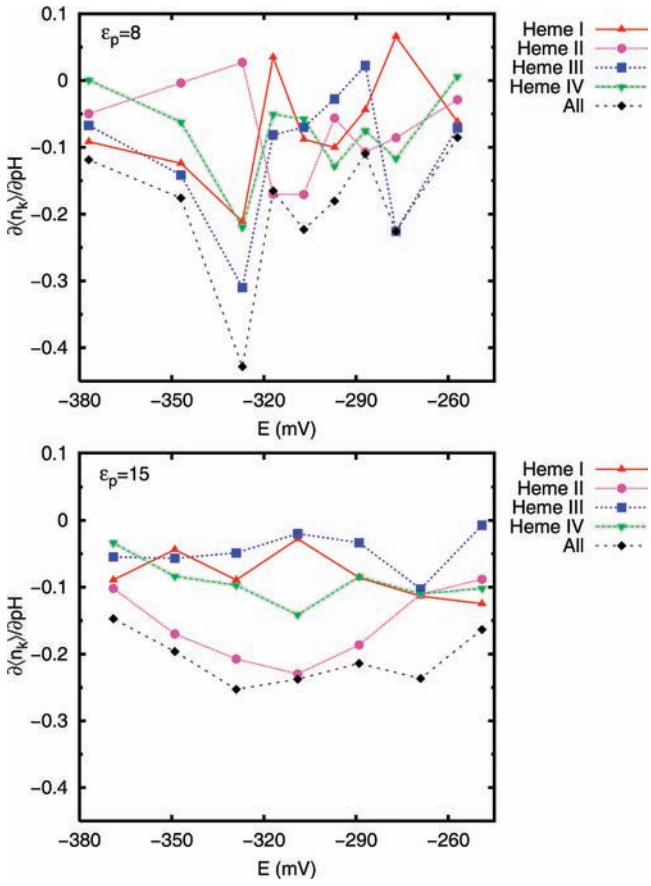

Figure 8. Heme reduction sensitivity toward pH at $\varepsilon_p = 8$ and 15.

good indication of the statistical reliability of the computed values. When a comparison is done with the experimental model,[59] the major discrepancy is the absence of any positive correlation (positive cooperativity) between hemes I and II. The same discrepancy was observed in our previous rigid-structure PB/MC studies,[21,66] where we suggested that it could be due to the lack of conformational rearrangements in the model; indeed, a negative correlation is what one would expect from purely electrostatic effects. However, the inclusion of conformational rearrangements in the present MD simulations does not change the coupling exhibited by hemes I and II. Since, as discussed above, there are no indications of insufficient structural reorganization in the simulations, these results suggest that either the protein experiences larger conformational changes at longer time scales or that the positive cooperativity reported in ref 59 between hemes I and II is an artifact of the fitting procedure. For the other correlations between heme centers, Figure 7 shows good agreement with the experimental model. The correlation observed with $\varepsilon_p = 15$ between heme II and His67 is also in good agreement with the large coupling indicated by the experimental model between this heme and the protonatable center. The experimental model also indicates a strong coupling between the protonatable center and heme I but, according to our previous rigid-structure PB/MC studies,[21,66] this probably corresponds to a interaction with the N-terminal amine; no such coupling can be observed in the present simulations because the titration of the N-terminal amine is statistically negligible at the simulation pH (6.6).

Despite the fact that all simulations were done at the same pH, it is possible to use the coupling between sites to measure the sensitivity of the reduction toward small pH changes (Figure 8). More exactly, we can measure how the average occupancy of a redox site is affected by pH, using the relation

$$\partial\langle n_k\rangle/\partial\mathrm{pH} = -\ln(10)(\langle n_k n_p\rangle - \langle n_k\rangle\langle n_p\rangle)$$

where n_k is the number of electrons in the heme group k, n_p is the total number of protons present in the sites allowed to titrate, and the angle brackets denote the ensemble average. Figure 8 shows that the slopes tend to be negative, corresponding to positive correlations between reduction and protonation, as one would expect from the mutual electrostatic stabilization of electrons and protons. In particular, the slope of the total reduction curve (given by the sum of the individual slopes) is always negative. Heme II is the most sensitive to pH changes (especially with $\varepsilon_p = 15$), reflecting its correlation with the nearby His67, as already discussed above. The points of high sensitivity displayed by hemes I, III, and IV with $\varepsilon_p = 8$ can be traced back to correlations with their propionates, but as noted

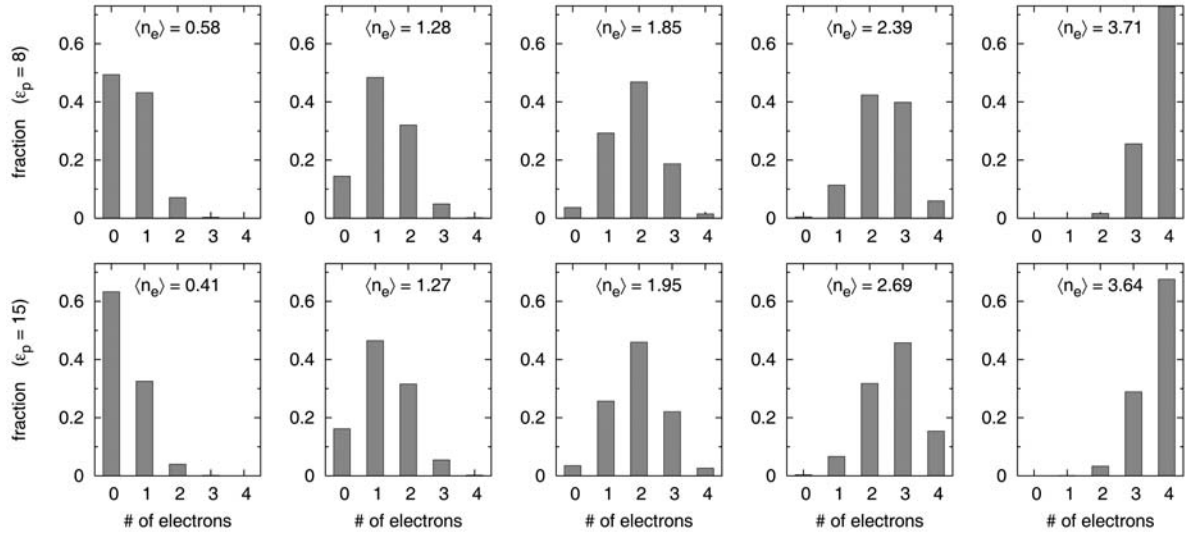

Figure 9. Histograms of electron populations at different average reduction ($\langle n_e\rangle$) for $\varepsilon_p = 8$ and 15. The reduction values range from 0 (fully oxidized) to 4 (fully reduced). The plots correspond from left to right: $E = -260$, -290, -310, -330, and -380 mV for $\varepsilon_p = 8$ and $E = -230$, -270, -290, -310, and -350 mV for $\varepsilon_p = 15$.

above, the propionate groups are scarcely titrating at the simulation pH leading to correlations affected by large sampling errors.

Electron Populations. Figure 9 shows the distribution of electron populations at different reduction potentials. It is clear that more hemes are reduced as the reduction potential becomes more negative, but the distribution is always considerably wide. For example, at a reduction potential close to the global half reduction there are on average two electrons present, but the molecules with two electrons contribute with only half of the total protein population. As noted before,[21] these large fluctuations on the number of electrons may play an important role in electron transfer under nonequilibrium conditions, since they allow the molecule to accommodate a "deficit" or "excess" of electrons from the kinetic viewpoint.

Concluding Remarks. This work presents a new implementation and extension of the stochastic titration method,[31] until now used to perform MD simulations at constant pH.[34−36] The present extension makes it possible to perform MD simulations at constant pH and *E*. The resulting constant-(pH,*E*) MD method allows for a joint sampling of protein conformations, solvent configurations, protonation states, and redox states, not possible with previous methods. As far as we know, this is the first implementation and application of a constant-(pH,*E*) MD method.

The present application of the method to cytochrome c_3 of *Desulfovibrio vulgaris* Hildenborough is a challenging test because the overall range of the midpoint reduction potentials of the hemes is close to the expected error of the method. A major finding of this study is that the method shows a better performance when the protein region is assigned a high ε_p, contrary to the theoretical expectation.[31] This is due to excessively high heme−heme interactions at low ε_p and markedly contrasts with the use of the method for constant-pH MD, where no such ε_p dependence was observed.[36] As discussed above, this indicates that explicit reorganization is insufficient, probably due to nonstructural responses (e.g., charge redistribution) not captured by the present method. When this lack of reorganization is accounted for by the use of a $\varepsilon_p = 8$ or 15, the reduction order is properly reproduced for three of the four heme groups (heme III is always out of order). We plan to investigate the nature of this insufficient reorganization in future work.

The simulations also reveal a strong coupling between hemes in close proximity, in good agreement with previous rigid-structure PB/MC calculations[21,66] and with an experimentally derived 5-site model,[59] except for the fact that no evidence was found for any positive cooperativity between hemes I and II. Furthermore, we show how the couplings can be used to estimate the sensibility of the heme reductions to small pH changes, despite the fact that the simulations are done at a single pH value. We also show that the partially reduced protein can easily accommodate a number of titrating electrons below or above its average value, which may be relevant under nonequilibrium conditions.

The present extension of the stochastic titration method to deal with reduction events can in principle be generalized to other methods currently used for constant-pH MD simulations. Hopefully, the pH and reduction potential of the solution will become standard external parameters in MD simulations.

Acknowledgment. We thank Cláudio Soares and Sara Campos for helpful discussions, and we acknowledge financial support from Fundação para a Ciência e Tecnologia, Portugal, through Grant Nos. SFRH/BPD/14540/2003, SFRH/BPD/29358/2006, and POCTI/BME/45810/2002.

Supporting Information Available: Figures S1−S3 showing temporal evolution of the shifting average of the secondary structure, RMSD values from the crystal structure of each amino acid residue, and a schematic respresentation of the differences between the X-ray structure and the average obtained from one of the simulations. This material is available free of charge via the Internet at http://pubs.acs.org.

JA808463E